

## VERY LONG BASELINE INTERFEROMETRY MEASURED PROPER MOTION AND PARALLAX OF THE $\gamma$ -RAY MILLISECOND PULSAR PSR J0218+4232

YUANJIE DU<sup>1,2</sup>, JUN YANG<sup>3</sup>, ROBERT M. CAMPBELL<sup>3</sup>, GEMMA JANSSEN<sup>4,5</sup>, BEN STAPPERS<sup>4</sup> AND DING CHEN<sup>1,2</sup>

*Published in The Astrophysical Journal Letters (Du et al. 2014, ApJL, 782, L38)*

### ABSTRACT

PSR J0218+4232 is a millisecond pulsar (MSP) with a flux density  $\sim 0.9$  mJy at 1.4 GHz. It is very bright in the high-energy X-ray and  $\gamma$ -ray domains. We conducted an astrometric program using the European VLBI Network (EVN) at 1.6 GHz to measure its proper motion and parallax. A model-independent distance would also help constrain its  $\gamma$ -ray luminosity. We achieved a detection of signal-to-noise ratio  $S/N > 37$  for the weak pulsar in all five epochs. Using an extragalactic radio source lying 20 arcmin away from the pulsar, we estimate the pulsar's proper motion to be  $\mu_\alpha \cos \delta = 5.35 \pm 0.05$  mas yr<sup>-1</sup> and  $\mu_\delta = -3.74 \pm 0.12$  mas yr<sup>-1</sup>, and a parallax of  $\pi = 0.16 \pm 0.09$  mas. The very long baseline interferometry (VLBI) proper motion has significantly improved upon the estimates from long-term pulsar timing observations. The VLBI parallax provides the first model-independent distance constraints:  $d = 6.3^{+8.0}_{-2.3}$  kpc, with a corresponding  $3\sigma$  lower-limit of  $d = 2.3$  kpc. This is the first pulsar trigonometric parallax measurement based solely on EVN observations. Using the derived distance, we believe that PSR J0218+4232 is the most energetic  $\gamma$ -ray MSP known to date. The luminosity based on even our  $3\sigma$  lower-limit distance is high enough to pose challenges to the conventional outer gap and slot gap models.

*Subject headings:* astrometry – pulsars: general – pulsars: individual (PSR J0218+4232)

### 1. INTRODUCTION

PSR J0218+4232 is a pulsar with a spin period of 2.3 millisecond and a period derivative of  $8.0 \times 10^{-20}$  s s<sup>-1</sup>. This millisecond pulsar (MSP) was first discovered by Navarro et al. (1995) using the Lovell telescope. The radio timing observations also found that it has a low-mass companion ( $M \gtrsim 0.16 M_\odot$ ) with an orbital period of 2 days. Optical observations using the Keck telescope revealed that the companion is a helium-core white dwarf with a temperature of  $T_{\text{eff}} = 8060 \pm 150$  K, and a distance constraint of 2.5–4 kpc is given by white-dwarf modeling (Bassa et al. 2003). Note that the distance uncertainty derived by this method is difficult to quantify exactly, because it is dependent on the white-dwarf's mass and optical luminosity, which are both correlated with the cooling age that is highly uncertain for observations and theoretical white-dwarf models (Bassa et al. 2003).

PSR J0218+4232 is also an energetic pulse emitter in X-rays and  $\gamma$ -rays. It was a  $\gamma$ -ray MSP candidate detected by Energetic Gamma Ray Experiment Telescope (Kuiper et al. 2000). Soon after *Fermi Gamma-ray Space Telescope* was launched, its was confirmed as a  $\gamma$ -ray MSP (Abdo et al. 2009). The X-ray pulsed emission has also been well detected and monitored by many X-ray telescopes (Webb et al. 2004). Currently, there are approximately 150 rotation-powered pulsars detected in the X-ray band, and about 50 of those have millisecond spin periods (Becker 2009). PSR J0218+4232 is

one of a few pulsars with a flux  $> 10^{-5}$  photon cm<sup>-2</sup> s<sup>-1</sup> in the 2 – 10 keV band (e.g., Kuiper et al. 2002). An absolute X-ray timing accuracy of  $\sim 200$   $\mu$ s was achieved by *Chandra* (Kuiper et al. 2004) and 40  $\mu$ s by *XMM-Newton* (Webb et al. 2004).

Astrometric parameters (e.g. position, proper motion, parallax) can be determined from pulsar timing observations over a time span of several years. It is still a challenge to measure the times of arrival of its pulses with a high precision since PSR J0218+4232 has broad profile and significant ( $\sim 50\%$ ) non-pulsed emission (Navarro et al. 1995). The best timing solution published to date was derived from observations at Effelsberg (Lazaridis 2009). The proper motion derived from these observations is  $\mu_\alpha \cos \delta = +5.1 \pm 0.3$  mas yr<sup>-1</sup> and  $\mu_\delta = -2.3 \pm 0.7$  mas yr<sup>-1</sup>, whose uncertainties are better than the previously published values in Hobbs et al. (2005). Furthermore, due to the occurrence of sources of timing noise in the time-of-arrival data (e.g., the pulsar's intrinsic spin-down noise, noise induced by the stochastic gravitational wave background, dispersion measure (DM) variations) as well as a relatively short timespan of timing observations that can lead to covariances with other parameters of the timing model, the pulsar-timing method can lead to significant errors in the estimated astrometric parameters.

The proper motion and trigonometric parallax of a pulsar can also be independently measured with VLBI observations. The high-precision VLBI astrometry has been applied to many bright slow pulsars (e.g., Campbell et al. 1996; Brisken et al. 2002, 2003; Chatterjee et al. 2009), and MSPs, such as PSR B1937+21 (Dewey et al. 1996), PSR J0437–4715 (Deller et al. 2008), and PSR B1257+12 with three planets (Yan et al. 2013). A pulsar distance measured to 0.4% accuracy has been recently achieved in the VLBI astrometry of PSR J2222–0137 (Deller et al. 2013). Astrometric parameters derived from VLBI observations can further improve the estimation of parameters from long-term pulsar timing observations, by providing a prior constraint on

<sup>1</sup> National Space Science Center, Chinese Academy of Sciences, No.1 Nanertiao, Zhongguancun, Haidian district, Beijing 100190, China; duyj@nssc.ac.cn

<sup>2</sup> Key Laboratory of Electronics and Information Technology for Space Systems, CAS

<sup>3</sup> Joint Institute for VLBI in Europe, Postbus 2, 7990 AA Dwingeloo, The Netherlands

<sup>4</sup> University of Manchester, Jodrell Bank Observatory, Macclesfield, Cheshire, SK11 9DL, UK

<sup>5</sup> ASTRON, the Netherlands Institute for Radio Astronomy, Postbus 2, 7990 AA, Dwingeloo, The Netherlands

astrometric parameters to which the timing analysis is insensitive, but which may themselves be highly covariant with other parameters uniquely approachable via timing. Combining VLBI- and timing-derived astrometry can contribute to frame ties between the International Celestial Reference Frame and the dynamical solar-system frame, which underlie VLBI and pulsar timing, respectively (Madison et al. 2013).

In this Letter, we present the results of the first VLBI observations of PSR J0218+4232. We summarize the strategy of the VLBI observations and the post-correlation data reduction in Section 2. We discuss the estimation of the pulsar’s astrometric parameters in Section 3. Finally, we address the model constraints on the  $\gamma$ -ray luminosity of the pulsar in Section 4.

## 2. VLBI OBSERVATIONS AND DATA REDUCTION

We conducted five epochs of European VLBI Network (EVN) observations of PSR J0218+4232 from 2010 November to 2012 October. The first three columns of Table 1 describe the basic characteristics of each epoch: observing date, participating telescopes (abbreviations listed in the note to the table), and recording bandwidth. All observations used 2-bit Nyquist sampling in both right- and left-circular polarizations (thus 1024 Mbps spans 128 MHz on the sky per polarization). The central frequency for each epoch was 1658.49 MHz. Each epoch lasted 6 hr. The remaining columns in Table 1 describe imaging results, which we will discuss later.

The EVN observations were done in the phase-referencing mode with a cycle time  $t_{\text{cyc}} \sim 6$  minutes, with a cycle typically comprising 80 s on the phase-reference source and 260 s on the target pulsar, plus gaps for system-temperature measurements. We used J0216+4240 as the main phase-reference source. This lies 20 arcmin away from the pulsar and has a compact-double structure with a total flux density  $154 \pm 15$  mJy at 1.6 GHz. Secondary phase-reference sources included J0228+4212 and J0222+4302 (3C66A), which were observed for a single 1-minute scan every 15 minutes. In our first epoch, we measured the position of the brighter northern component of the main phase-reference source ( $\alpha_{\text{J2000}} = +02^{\text{h}}16^{\text{m}}25^{\text{s}}972281$ ,  $\delta_{\text{J2000}} = +42^{\circ}40'36''.42857$ ) with respect to J0222+4302. The  $1\sigma$  absolute position uncertainty for J0222+4302 is  $\sim 0.05$  mas from the GSFC geodetic solution 2009a (NASA Goddard Space Flight Center VLBI Group 2009). We continued to use this northern component in J0216+4240 as the reference point to track the relative position variation of the pulsar in all five epochs. Despite its proximity to the pulsar on sky, it was still too far to gain the benefits of using it as an in-beam calibrator. The FWHM (the full width at half maximum of the synthesized beam) of the several 32m telescopes in the EVN would be about 4% less than the separation, and the larger, more sensitive telescopes would certainly need to be slewed. The 76m Jodrell Bank Lovell telescope (Jb1) has slewing limitations ( $\sim 12$  source changes per hour) that require adjustments in the phase-reference scheduling when the  $t_{\text{cyc}}$  is under 10 minutes. The standard tactic is to omit Jb1 from every other phase-reference source scan, which in the present case yielded an apparent  $t_{\text{cyc}}$  of  $\sim 12$  minutes for it.

Correlation was performed using the EVN software correlator at JIVE (SFXC). The position of the pulsar used for correlation was  $\alpha_{\text{J2000}} = +02^{\text{h}}18^{\text{m}}06^{\text{s}}3580062$ ,  $\delta_{\text{J2000}} = +42^{\circ}32'17''.379133$ . Pulsar gating during correlation is a technique in which only a specified portion of the pulse period is actually correlated, typically providing a signal-to-noise ra-

tio (S/N) gain on the order of the inverse square-root of the pulsar’s duty cycle (i.e., assuming no off-pulse emission). Gating was not applied during these correlations because of the pulsar’s broad pulse and significant off-pulse emission (Navarro et al. 1995).

The data were calibrated using the NRAO Astronomical Image Processing System (Greisen 2003). The correlation amplitude was calibrated initially with measured system temperatures and antenna gain curves for telescopes having reliable data, and with nominal system equivalent flux density values for other telescopes. The ionospheric delay was corrected via the total electron content measurements from GPS monitoring. Phase contributions from the antenna parallactic angle were removed before fringe fitting. The phase bandpass solutions were determined from all the calibrator data. Some stations had bandpasses characterized by a sharp cut-off  $\sim 1.5$  MHz from the band-edge on each side. Since the astrometry is based primarily on the phases, we did not apply amplitude bandpass solutions to avoid introducing noise from these band-edge channels when spectral averaging across the bands. The calibrator was imaged in Difmap (Shepherd et al. 1994), using the observations in the final epoch, which was the most sensitive one. The phase contribution arising from the calibrator source structure was subtracted via re-running the fringe fitting. We did not see any significant flux or structure variations in the calibrator over the epochs. The pulsar position was derived in Difmap (Shepherd et al. 1994) through fitting the visibility data to a point-source model. Data from Jb1 in the fourth epoch were ultimately omitted: the combination of its longer apparent  $t_{\text{cyc}}$  ( $\sim 720$  s) arising from its slewing limitations as discussed above and higher residual phase rate in this epoch ( $\sim 2.5$  mHz) led to a less reliable phase-connection.

Columns 4–10 of Table 1 characterize the imaging results of the five epochs. Columns 4–6 show the geometry of the naturally-weighted restoring beam. Columns 7–8 give the total flux density and dynamic range (S/N) of the pulsar images. Columns 9–10 list the residual position of the pulsar with  $1\sigma$  formal errors  $\frac{\text{FWHM}}{2\text{S/N}}$ . We typically achieved an image sensitivity of  $\sim 12 \mu\text{Jy beam}^{-1}$  (natural weighting) in the epochs having a total bandwidth of 1024 Mbps. PSR J0218+4232 was detected with a S/N  $> 37$  in each of the five epochs.

## 3. EVN ASTROMETRY OF PSR J0218+4232

Using least-squares (L-S) minimization, we estimated the standard five astrometric parameters for the pulsar from its observed residual positions. These five parameters are the J2000 position at the reference epoch 2011.7893 ( $\alpha_0$ ,  $\delta_0$ ), proper motion ( $\mu_\alpha \cos \delta$ ,  $\mu_\delta$ ), and parallax ( $\pi$ ). Table 2 lists the results of the L-S fitting. The reduced chi-square of this fit was 0.72 (for five degrees of freedom). The right-hand panel of Figure 1 plots the  $1\sigma$  error ellipses for the pulsar’s position at each epoch and its motion on the plane of the sky computed from the estimated proper motion and parallax.

PSR J0218+4232 is moving toward the south-east at a position angle  $\sim 125^\circ$ . The magnitude of its proper motion is  $\mu_{\text{tot}} = 6.53 \pm 0.08 \text{ mas yr}^{-1}$ . Our VLBI proper motion estimate is consistent at a  $2\sigma$  level with the most recently published values from timing observations from Lazaridis (2009) ( $\mu_\alpha \cos \delta = +5.1 \pm 0.3 \text{ mas yr}^{-1}$  and  $\mu_\delta = -2.3 \pm 0.7 \text{ mas yr}^{-1}$ ), while the precision of the EVN estimate is a factor of six better.

Our marginally significant measurement of the parallax,

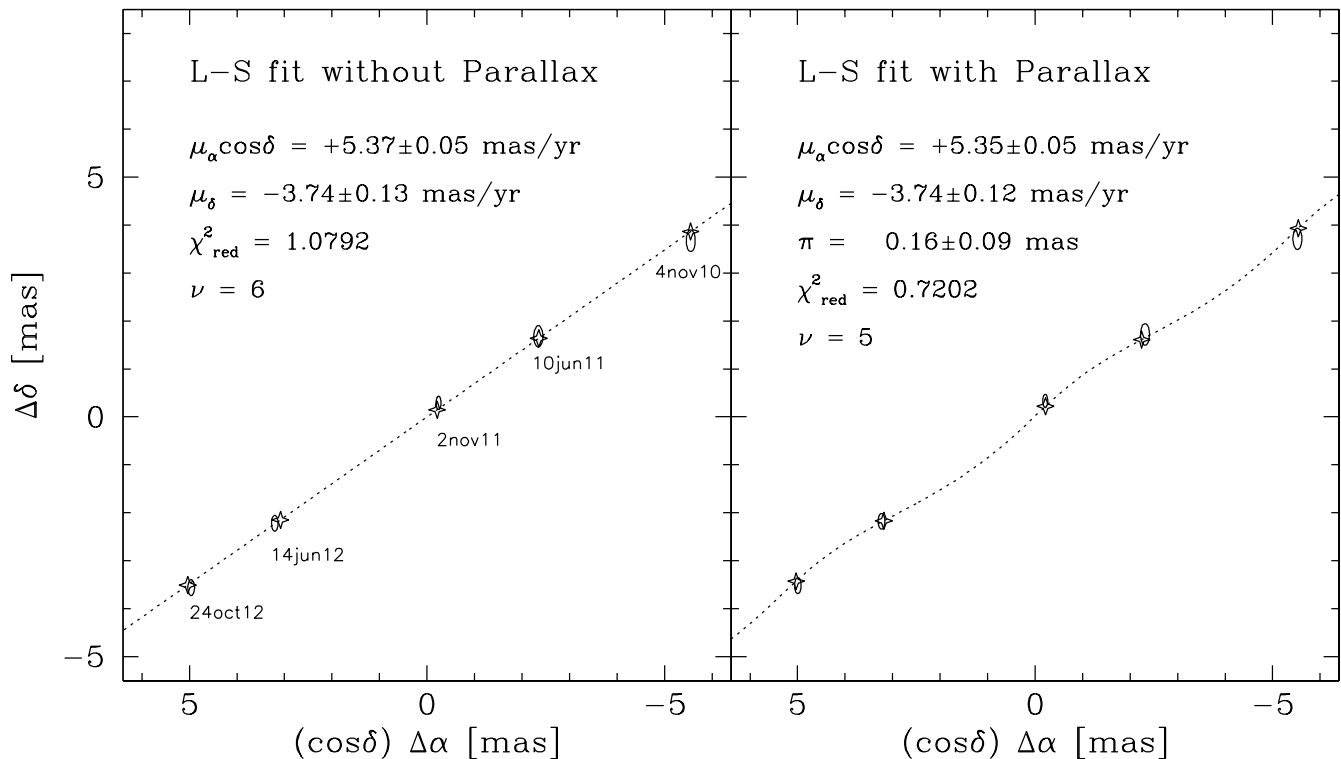


FIG. 1.— EVN astrometry: PSR J0218+4232 positions,  $1\sigma$  error ellipses, and the modeled track in the sky plane. A star symbol denotes the calculated pulsar position at the epoch of each observing session. The origin gives the position derived at the reference epoch J2011.8793. Some results from the least-squares fit are annotated in each panel. Table 2 lists the results for the fit that includes parallax.

TABLE 1  
SUMMARY OF THE EVN OBSERVATIONS AND IMAGING RESULTS OF THE PSR J0218+4232

MJD (day)	Participating Telescopes	Bandwidth (Mbps)	$\theta_{\text{maj}}$ (mas)	$\theta_{\text{min}}$ (mas)	$\theta_{\text{pa}}$ (deg)	$S_{\text{tot}}$ (mJy)	$S_{\text{peak}}/\sigma_{\text{rms}}$	$\Delta\alpha \cos\delta$ (mas)	$\Delta\delta$ (mas)
55504.811	Ef, Wb, On, Tr, Mc, Sv, Zc, Bd, Jb2	512	19.0	8.03	4.79	0.61	42.5	$0.65 \pm 0.09$	$-0.26 \pm 0.22$
55722.223	Ef, Wb, On, Tr, Mc, Sv, Zc, Bd, Jb1, Ur, Sh	1024	16.8	7.07	7.16	0.45	37.6	$3.86 \pm 0.09$	$-2.25 \pm 0.22$
55867.834	Ef, Wb, On, Tr, Mc, Sv, Zc, Bd, Jb1, Ur, Sh	1024	14.0	5.33	7.61	0.59	51.2	$5.96 \pm 0.05$	$-3.64 \pm 0.14$
56092.209	Ef, Wb, On, Tr, Mc, Sv, Zc, Bd, Jb1, Ur, Sh, Nt	1024	14.7	6.21	7.69	0.57	42.5	$9.41 \pm 0.07$	$-6.15 \pm 0.16$
56224.917	Ef, Wb, On, Tr, Mc, Sv, Zc, Bd, Jb2, Ur, Sh, Nt, Ro70	1024	15.8	6.58	-15.5	0.51	47.8	$11.2 \pm 0.07$	$-7.49 \pm 0.16$

NOTE. — Ef: Effelsberg, Wb: Westerbork Synthesis Radio Telescope (WSRT) in phase-array mode, On: Onsala 25 m, Tr: Torun, Mc: Medicina, Sv: Svetloe, Zc: Zelenchukskaya, Bd: Badary, Jb1: Jodrell Bank Lovell telescope, Jb2: Jodrell Bank Mark2 telescope, Ur: Urumqi, Sh: Shanghai, Nt: Noto, Ro70: Robledo 70 m

TABLE 2  
VLBI ASTROMETRY OF THE PSR J0218+4232.

Fitting parameter	Best-fit value
R.A., $\alpha_0$ (J2000)	$02^{\text{h}}18^{\text{m}}06^{\text{s}}.358569 \pm 0^{\text{s}}.000002$
Decl., $\delta_0$ (J2000)	$42^{\circ}32'17''.37515 \pm 0''.00008$
Proper motion in R.A., $\mu_{\alpha} \cos\delta$	$5.35 \pm 0.05 \text{ mas yr}^{-1}$
Proper motion in Decl., $\mu_{\delta}$	$-3.74 \pm 0.12 \text{ mas yr}^{-1}$
Parallax, $\pi$	$0.16 \pm 0.09 \text{ mas}$

$\pi = 0.16 \pm 0.09$  mas, corresponds to a distance of  $d = 6.3^{+8.0}_{-2.3}$  kpc, and to a  $3\sigma$  lower-limit to  $d$  of 2.3 kpc. Currently, there is no distance estimation available from timing observations, making this is the first model-independent distance measurement. The uncertainty of the parallax estimation is reasonable, compared with astrometric results using a reference source at a similar angular separation (Deller et al. 2013). Because the significance of the parallax-parameter estimate in the L-S fit is only at the  $2\sigma$  level, we also fit a model without parallax. The left-hand panel of Figure 1 shows the results of this fit. It can be seen that the estimated proper-motion components are insensitive to exclusion of parallax from the model. Furthermore, we can integrate

the  $F$ -distribution formed by the ratio of the chi-square to variate with the appropriate number of degrees of freedom, resulting from the two fits in order to characterize the significance of the parameter ( $\pi$ ) in one of the models (e.g., Bevington 1969; Stuart & Ord 1994). Such a test shows that we can reject the exclusion of the parallax parameter at only a 34% confidence level, this is also consistent with the VLBI data not being able to constrain  $\pi$  strongly. The transverse velocity derived from the proper motion and parallax is  $V_{\text{T}} = 4.74\mu_{\text{tot}}/\pi = 195^{+249}_{-71} \text{ km s}^{-1}$ , with the uncertainty dominated by  $\sigma_{\pi}$ . The statistical mean value of  $\bar{V}_{\text{T}}$  for MSPs as a whole is  $87 \pm 13 \text{ km s}^{-1}$  (Hobbs et al. 2005). It seems that PSR J0218+4232 has a large transverse velocity among MSPs.

A model-dependent distance for a pulsar can be derived from its DM and a Galactic electron density ( $n_{\text{e}}$ ) model. A set of distances derived from VLBI trigonometric parallaxes can provide point calibrations to models of Galactic  $n_{\text{e}}$ . In the case of this MSP, with a DM of  $61.25 \text{ pc cm}^{-3}$  (Navarro et al. 1995), the TC model (Taylor & Cordes 1993) yields a distance of 5.7 kpc and the NE2001 model (Cordes & Lazio 2002) a distance of 2.7 kpc. Thus, the distance obtained from



the TC model is more consistent with our parallax-based distance in this case.

The Doppler correction to the spin-down luminosity  $\dot{E}$  of PSR J0218+4232 is small. The apparent period derivative  $\dot{P}_{\text{shk}}$  due to the ‘‘Shklovskii effect’’ (Shklovskii 1970) is

$$\dot{P}_{\text{shk}} = \frac{V_{\text{r}}^2 P}{dc} = 1.5 \times 10^{-21},$$

where  $c$  is the speed of light,  $P$  the rotation period of a pulsar.  $\dot{P}_{\text{shk}}$  is thus only a small fraction ( $\sim 1.9\%$ ) of the total  $\dot{P} = 7.74 \times 10^{-20} \text{ s s}^{-1}$ . In addition, we estimated the  $\dot{P}_{\text{gal}}$  induced by Galactic rotation, and it is much smaller than  $\dot{P}_{\text{shk}}$ . Therefore, both  $\dot{P}_{\text{shk}}$  and  $\dot{P}_{\text{gal}}$  can be ignored, and the intrinsic spin-down  $\dot{P}$  dominates the total period derivative.

The uncertainties of the estimated pulsar position at the reference epoch in Table 2 are statistical errors from the fit. The phase connections between J0216+4240 and PSR J0218+4232 worked quite well and there was no significant red noise (e.g., striping) in the clean image. This is also as expected from the high declination and quite small separation (20 arcmin) between these two sources. Thus, the main systematic position error arises from the phase connections between J0222+4302 and J0216+4240 separated by  $1.^\circ 2$ . The absolute position error of J0222+4302 is  $1\sigma = 0.05$  mas from the geodetic VLBI solution GSFC2009a (NASA Goddard Space Flight Center VLBI Group 2009). Using J0216+4240 as the reference source, we also checked the variation of J0222+4302 position in these multi-epoch experiments. The resulting uncertainty in the derived J0222+4302 position, mainly caused by the ionosphere propagation effect, is  $1\sigma = 0.2$  mas. Combining these two factors in quadrature, the measurement of the systematic position error at the reference epoch is  $1\sigma = 0.21$  mas.

#### 4. THE MOST LUMINOUS $\gamma$ -RAY MSP?

There are 40 MSPs in the second Fermi Large Area Telescope Catalog of  $\gamma$ -ray pulsars (Abdo et al. 2013). PSR J0218+4232 is one of a few strong  $\gamma$ -ray MSPs. Its  $\gamma$ -ray (0.1–100 GeV) energy flux is  $F = 4.56 \times 10^{-11} \text{ erg s}^{-1} \text{ cm}^{-2}$ . Abdo et al. (2013) calculated its luminosity,  $L_{\gamma} = 4\pi f_{\Omega} F d^2 \approx 3.8 \times 10^{34} \text{ erg s}^{-1}$ , based on a DM distance  $d = 2.6$  kpc and a beaming fraction  $f_{\Omega} = 1$ .

In Figure 2, we re-plot  $\gamma$ -ray luminosity  $L_{\gamma}$  versus spin-down luminosity  $\dot{E}$  of the 40 MSPs. Using our parallax-based distance (6.3 kpc) and assuming  $f_{\Omega} = 1$ , PSR J0218+4232 has a luminosity  $L_{\gamma} \approx 2.2 \times 10^{35} \text{ erg s}^{-1}$ , a factor of six higher than the previous measurement. This makes it the most energetic  $\gamma$ -ray MSP. Its spin-down luminosity is  $\dot{E} = 2.4 \times 10^{35} \text{ erg s}^{-1}$ . Combining its  $\dot{E}$  and  $L_{\gamma}$ , the pulsar has a  $\gamma$ -ray efficiency  $\eta = L_{\gamma}/\dot{E} \sim 92\%$ , which, while in the reasonable range, is still quite high. Even if we use the  $3\sigma$  lower-limit distance, the corresponding luminosity is  $L_{\gamma,3\sigma} \approx 3.0 \times 10^{34} \text{ erg s}^{-1}$ , and PSR J0218+4232 is still one of the three most luminous MSPs in the  $\gamma$ -ray band.

Below, we discuss the high luminosity that we compute with the  $3\sigma$  lower-limit distance of PSR J0218+4232 in the context of three emission models: the outer gap model, the slot gap model, and the annular gap model.

The outer gap model is a popular high-energy emission model, which can explain emission mechanism for MSPs (Cheng 2013). He gives a convenient formula with which to

estimate the  $\gamma$ -ray luminosity  $L_{\gamma, \text{OG}}$  for MSPs:

$$L_{\gamma, \text{OG}} \simeq f_{\text{gap}}^3 \dot{E},$$

where

$$f_{\text{gap}} = 5.5 P^{26/21} B_{12}^{-4/7}$$

is the fractional size of the outer gap and  $B_{12} = 4.29$  (Manchester et al. 2005) is the surface magnetic field in units of  $10^{12}$  G. When taking the relevant values of PSR J0218+4232 into the formulae above, the derived  $\gamma$ -ray luminosity from the outer gap model is  $L_{\gamma, \text{OG}} = 3.9 \times 10^{33} \text{ erg s}^{-1}$ , which is much smaller than  $L_{\gamma, 3\sigma}$ . Even if we consider the effects of both the magnetic inclination angle ( $\alpha$ ) and the emission geometry for the outer gap model as described in (Zhang et al. 2004) and (Jiang et al. 2014), the derived  $L_{\gamma, \text{OG}}$  remains smaller than  $L_{\gamma, 3\sigma}$ . For  $\alpha$  in the reasonable range of  $10^\circ - 90^\circ$ ,  $L_{\gamma, \text{OG}}$  is  $1.0 - 12.9 \times 10^{33} \text{ erg s}^{-1}$ , which is still smaller than  $L_{\gamma, 3\sigma}$ . To reach a compatible value with  $L_{\gamma, 3\sigma}$  for PSR J0218+4232, an unphysical value of  $30 - 2.3$  for  $\Delta\phi/\Delta\Omega$  would be required (Jiang et al. 2014). Here  $\Delta\phi$  and  $\Delta\Omega$  are the extension angle at azimuthal direction and  $\gamma$ -ray beaming solid angle, respectively.

The slot gap model, developed from the two-pole caustic model (Dyks & Rudak 2003), is another popular model to explain the high-energy emission from pulsars (Muslimov & Harding 2003, 2004). As described by Hard-

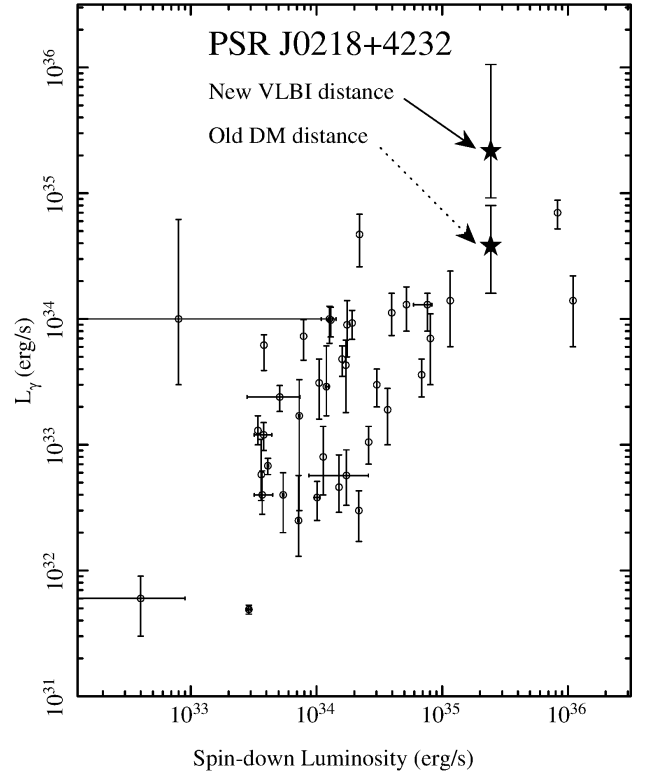


FIG. 2.—  $\gamma$ -ray luminosity  $L_{\gamma}$  in the 0.1–100 GeV energy band vs. spin-down luminosity  $\dot{E}$ . The data, except for PSR J0218+4232 (star symbol), are adopted from the second catalog of *Fermi*-LAT MSPs (Abdo et al. 2013) and are re-plotted here as a reference sample. Our new  $1\sigma$  parallax measurement supports that PSR J0218+4232 is the most energetic  $\gamma$ -ray MSP.

ing<sup>6</sup>, the  $\gamma$ -ray luminosity can be given by:

$$\begin{aligned} L_{\gamma,SG} &\approx 2 \times 10^{34} \epsilon_{\gamma} \dot{E}_{35}^{3/7} P_{0.1}^{5/7} \Omega_{SG} \text{ erg s}^{-1} \\ &\simeq 0.2 \times 10^{34} \epsilon_{\gamma} \Omega_{SG} \text{ erg s}^{-1}, \end{aligned}$$

where  $\epsilon_{\gamma} \lesssim 1$  a conversion efficiency factor parameterizing how much of the primary particle luminosity converts into  $\gamma$ -ray ( $> 100$  MeV) emission,  $\dot{E}_{35}$  is a pulsar's spin-down luminosity in units of  $10^{35} \text{ erg s}^{-1}$ ,  $P_{0.1}$  the spin period in units of 0.1 s, and  $\Omega_{SG}$  the solid angle ( $\leq 4\pi$ ) of the slot gap. For PSR J0218+4232, the derived value of  $L_{\gamma,SG}$  is smaller than  $L_{\gamma,3\sigma}$  even if  $\epsilon_{\gamma} \sim 1$  and  $\Omega_{SG} \sim 4\pi$  are adopted.

The annular gap model is a new model under development for treating multi-wavelength emission from pulsars (Qiao et al. 2004; Du et al. 2010). Qiao et al. (2007) gave an analytical formula of the primary particle luminosity  $L_{\text{prim,AG}}$  to the annular gap model<sup>7</sup>. Using a conversion efficiency factor  $\epsilon_{\gamma}$  for  $> 100$  MeV band, the  $\gamma$ -ray luminosity ( $L_{\gamma,AG}$ ) of PSR J0218+4232 in the annular gap model is

$$\begin{aligned} L_{\gamma,AG} &= \epsilon_{\gamma} L_{\text{prim,AG}} = \frac{16\pi^2 \epsilon_{\gamma} B^2 R^6}{c^3 P^4} (0.26 + 0.13\alpha)^2 \\ &\simeq 1.8 \times 10^{35} \epsilon_{\gamma} R_6^6 \text{ erg s}^{-1}, \end{aligned}$$

where  $R_6$  is the radius of a pulsar in units of  $10^6$  cm. In this model,  $L_{\gamma,AG}$  can reasonably fall within the range of allowable luminosities given our  $3\sigma$  lower-limit distance. Note that the  $\gamma$ -ray flux may be non-uniformly distributed in the emission beam, it could be varying with line of sight.  $f_{\Omega}$  is model-dependent, with  $f_{\Omega} \sim 0.2 - 0.8$  for MSPs in the annular gap model (Du et al. 2010, 2013).

Therefore, the high  $\gamma$ -ray luminosity derived from our  $3\sigma$  lower-limit distance for PSR J0218+4232 can be well explained by the annular gap model. However, the magnitude of the luminosity poses challenges for the outer gap model and the slot gap model in their current state.

The authors are grateful to the referee for constructive comments. We appreciate Li Guo for giving us some useful information. Y.J.D. is supported by China Postdoctoral Science Foundation (Grant No. 2012M510047) and the National Natural Science Foundation of China (Grant No. 11303069 and 11373011). The European VLBI Network is a joint facility of European, Chinese, South African and other radio astronomy institutes funded by their national research councils. This research has made use of NASA Goddard Space Flight Center's geodetic VLBI solution 2009a, ATNF Pulsar Catalogue and NASA's Astrophysics Data System.

#### REFERENCES

- Abdo, A. A., Ackermann, M., Ajello, M., et al. 2009, *Science*, 325, 848  
 Abdo, A. A., Ajello, M., Allafort, A., et al. 2013, *ApJS*, 208, 17  
 Bassa, C. G., van Kerkwijk, M. H., & Kulkarni, S. R. 2003, *A&A*, 403, 1067  
 Becker, W. 2009, *Astrophysics and Space Science Library*, 357, 91  
 Bevington, P. R. 1969, *Data Reduction and Error Analysis for the Physical Sciences* (New York: McGraw-Hill), §10.2  
 Briskin, W. F., Benson, J. M., Goss, W. M., & Thorsett, S. E. 2002, *ApJ*, 571, 906  
 Briskin, W. F., Fruchter, A. S., Goss, W. M., Herrnstein, R. M., & Thorsett, S. E. 2003, *AJ*, 126, 3090  
 Campbell, R. M., Bartel, N., Shapiro, I. I., Ratner, M. I., Cappallo, R. J., Whitney, A. R., & Putnam, N. 1996, *ApJ*, 461, L95  
 Chatterjee, S., Briskin, W. F., Vlemmings, W. H. T., et al. 2009, *ApJ*, 698, 250  
 Cheng, K. S. 2013, *Journal of Astronomy and Space Sciences*, 30, 153  
 Cordes, J. M., & Lazio, T. J. W. 2002, *arXiv:astro-ph/0207156*  
 Deller, A. T., Verbiest, J. P. W., Tingay, S. J., & Bailes, M. 2008, *ApJ*, 685, L67  
 Deller, A. T., Boyles, J., Lorimer, D. R., Kaspi, V. M., McLaughlin, M. A., Ranson, S., Stairs, I. H. & Stovall, K. 2013, *ApJ*, 770, 145  
 Dewey, R. J., Ojeda, M. R., Gwinn, C. R., Jones, D. L., & Davis, M. M. 1996, *AJ*, 111, 315  
 Du, Y. J., Qiao, G. J., Han, J. L., Lee, K. J., Xu, R. X. 2010, *MNRAS*, 406, 2671  
 Du, Y. J., Qiao, G. J., & Chen, D. 2013, *ApJ*, 763, 29  
 Dyks, J., & Rudak, B. 2003, *ApJ*, 598, 1201  
 Greisen, E. W., in Heck A., ed., *Astrophysics and Space Science Library* Vol. 285, *Information Handling in Astronomy: Historical Vistas*. Kluwer, Dordrecht, p. 109  
 Hobbs, G., Lorimer, D. R., Lyne, A. G., & Kramer, M. 2005, *MNRAS*, 360, 974  
 Jiang, Z. J., Chen, S. B., Li, X., & Zhang, L. 2014, *MNRAS*, 437, 2957  
 Kuiper, L., Hermsen, W., Verbunt, F., et al. 2000, *A&A*, 359, 615  
 Kuiper, L., Hermsen, W., Verbunt, F., et al. 2002, *ApJ*, 577, 917  
 Kuiper, L., Hermsen, W., & Stappers, B. 2004, *Advances in Space Research*, 33, 507  
 Lazaridis, K. 2009, PhD thesis, Univ. Koln  
 Madison, D. R., Chatterjee, S., & Cordes, J. M. 2013, *ApJ*, 777, 104  
 Manchester, R. N., Hobbs, G. B., Teoh, A., & Hobbs, M. 2005, *AJ*, 129, 1993  
 Muslimov, A. G., & Harding, A. K. 2003, *ApJ*, 588, 430  
 Muslimov, A. G., & Harding, A. K. 2004, *ApJ*, 606, 1143  
 Navarro, J., de Bruyn, A. G., Frail, D. A., Kulkarni, S. R., & Lyne, A. G. 1995, *ApJ*, 455, L55  
 NASA Goddard Space Flight Center VLBI Group, 2009. Data products available electronically at <http://gemini.gsfc.nasa.gov/solutions/2009a/>.  
 Qiao, G. J., Lee, K. J., Wang, H. G., Xu, R. X., & Han, J. L. 2004, *ApJ*, 606, L49  
 Qiao, G.-J., Lee, K.-J., Zhang, B., Wang, H.-G., & Xu, R.-X. 2007, *Chinese J. Astron. Astrophys.*, 7, 496  
 Shepherd M. C., Pearson T. J., & Taylor G. B. 1994, *BAAS*, 26, 987  
 Shklovskii, I. S. 1970, *Soviet Ast.*, 13, 562  
 Stuart, A. & Ord, J. K. 1994, *Kendall's Advanced Theory of Statistics*, Vol.1 (London: Hodder Arnold), §16.15  
 Taylor, J. H., & Cordes, J. M. 1993, *ApJ*, 411, 674  
 Webb, N. A., Olive, J.-F., & Barret, D. 2004, *A&A*, 417, 181  
 Yan, Z., Shen, Z.-Q., Yuan, J.-P., Wang, N., Rottmann, H., & Alef, W. 2013, *MNRAS*, 433, 162  
 Zhang, L., Cheng, K. S., Jiang, Z. J., & Leung, P. 2004, *ApJ*, 604, 317

<sup>6</sup> See the report of <http://www2011.mpe.mpg.de/363-heraeus-seminar/Contributions/2Tuesday/morning/AHarding.pdf>  
<sup>7</sup> There is a typo in Equation 6 of Qiao et al. (2007), where a factor of  $c^2$  is omitted in the denominator of  $\Phi_{\text{Max,ann}}$ .